Journal of Process Control 21 (2011) 194–204

Contents lists available at ScienceDirect

Journal of Process Control

journal homepage: www.elsevier.com/locate/jprocont

Min–Max MPC based on an upper bound of the worst case cost with guaranteed stability. Application to a pilot plant

J.K. Gruber*, D.R. Ramirez, T. Alamo, E.F. Camacho

Ingeniería de Sistemas y Automática, Escuela Superior de Ingenieros, Universidad de Sevilla, Camino de los Descubrimientos s/n, 41092 Seville, Spain

ARTICLE INFO

Article history:
Received 2 August 2010
Received in revised form
27 November 2010
Accepted 30 November 2010

Keywords:
Min–Max Model Predictive Control
Uncertain linear systems
Continuous stirred tank reactor

ABSTRACT

Min–Max MPC (MMMPC) offers the possibility to consider disturbances and uncertainties in the mathematical model used to predict the future trajectory of the system. The explicit consideration of disturbances and uncertainties in order to obtain a more robust control performance complicates the practical implementation of MMMPC due to the high computational burden required to compute the control law. The computational complexity of the optimization problem can be reduced by using approximate solutions or upper bounds of the worst case cost of the objective function. A computationally efficient MMMPC strategy based on such an upper bound was presented in a previous work also published in this journal (see Section 1). One of the main drawbacks of that strategy is the lack of a stability guarantee. In this paper it is shown that input-to-state practical stability of the MMMPC strategy can be guaranteed if a certain initial condition and a semi-feedback approach are used. Furthermore, the MMMPC strategy is validated in experiments with a continuous stirred tank reactor in which the temperature of the reactor is controlled. The behavior of the system and the controller are illustrated by means of experimental results.

1. Introduction

Min–Max Model Predictive Control (MMMPC) offers the possibility to consider disturbances and model uncertainties in the prediction model within the framework of Model Predictive Control (MPC). In MMMPC strategies, the optimal control signal is computed minimizing the worst case cost. The mentioned worst case cost can be calculated maximizing the considered cost function with respect to all possible cases of disturbances and uncertainties [1,2]. The main drawback of this approach is the computational burden required to calculate the control signal by solving the resulting optimization problem. The optimization usually includes the solution of an NP-hard problem [3,4]. As a consequence of the numerical complexity to determine the control signal, the number of applications of MMMPC strategies is very small, even when there is evidence that they work better than standard MPC strategies in processes with uncertain dynamics or disturbances [5].

It is well known that the MMMPC control law based on linear models is piecewise affine when a 1-norm [6,7] or quadratic [8] criterion is used in the cost function. This property enables the possibility to build explicit forms of the control law with a reduced complexity [9]. Such explicit forms can be evaluated very fast provided that the complexity of the state space partition is moderate, which is the case for many applications. However, if the process model or the controller tuning parameters change, the computation of the controller has to be redone.

In Ref. [10], a computationally efficient MMMPC strategy in which the worst case cost is approximated by an upper bound has been presented. This strategy is based on a diagonalization algorithm which has a much lower computational burden than LMI techniques which have been proposed to obtain upper bounds [11,12]. The mentioned algorithm uses only simple matrix operations and can be implemented even with programming languages not destined for mathematical calculations, commonly found in industrial embedded systems. However, one of the main drawbacks of that strategy is the lack of a stability guarantee.

In this work, input-to-state practical stability is proven for the MMMPC strategy presented in Ref. [10]. Stability of the mentioned MMMPC strategy is guaranteed for a certain initial condition in the optimization procedure and under consideration of a semi-feedback approach [13]. Furthermore, the control strategy is validated in experiments with a continuous stirred tank reactor (CSTR). The used system emulates the heat produced by an exothermic chemical reaction using an electric resistance. It has been used before as a benchmark system for nonlinear and Min–Max Model Predictive Control strategies [14,15]. The nonlinear process dynamics are approximated by means of a linear model with additive and bounded uncertainties. The MMMPC strategy is implemented with the identified model and robustness of the control strategy can be

* Corresponding author. Tel.: +34 954 488 161; fax: +34 954 487 340.
E-mail addresses: jgruber@cartuja.us.es, jorngruber@gmail.com (J.K. Gruber).

0959-1524/$ – see front matter © 2010 Elsevier Ltd. All rights reserved.
doi:10.1016/j.jprocont.2010.11.016

shown with the help of experimental results. The use of an upper bound of the worst case cost considerably reduces the computational burden of the optimization problem and, as a consequence, allows to employ realistic values for the prediction horizon. It has to be mentioned that the personal computer used to implement the MMMPC strategy based on an upper bound of the worst case cost has not enough computing power to solve the exact min–max optimization problem within a reasonable time. The results obtained in setpoint tracking and disturbance rejection experiments prove the validity and underline the robustness of the control strategy. A direct comparison of the results shows that the MMMPC strategy performs better than a standard MPC based on the same prediction model and controller parameters (but without additive uncertainty). The low computational burden, the stability guarantee and the simplicity of the tuning parameters suggest that the proposed strategy is a possible alternative to traditional nominal MPC schemes.

The outline of the paper is the following: Section 2 defines the general min–max optimization problem. Section 3 presents the computation of the upper bound of the worst case cost and the resulting control law. In Section 4 input-to-state practical stability of the MMMPC strategy is proven. Section 5 gives a description of the used continuous stirred tank reactor and Section 6 presents the obtained experimental results. Finally, the major conclusions are drawn in Section 7.

2. Min–Max MPC with bounded additive uncertainties

Consider the following discrete-time state space model with a bounded additive uncertainty [5]:

$$\begin{aligned} x(k+1) &= Ax(k) + Bu(k) + D\theta(k) \\ y(k) &= Cx(k) \end{aligned} \tag{1}$$

where $x(K) \in \mathbb{R}^{n_x}$ denotes the state vector, $u(K) \in \mathbb{R}^{n_u}$ represents the input vector and $\theta(k) \in \{\theta \in \mathbb{R}^{n_\theta} : \left\|\theta\right\|_\infty \leq \varepsilon\}$ is the bounded uncertainty. The system is subject to n_c state and input time-invariant constraints $F_u u(k) + F_x x(k) \leq b_c$ where $F_u \in \mathbb{R}^{n_c \times n_u}$ and $F_x \in \mathbb{R}^{n_c \times n_x}$. Furthermore, the input signal is given by a semi-feedback approach [13]:

$$u(k) = -Kx(k) + v(k) \tag{2}$$

where $v(k)$ denotes the input correction vector and the feedback matrix K is chosen to achieve some desired property such as nominal stability or linear quadratic regulator (LQR) optimality without constraints. With the semi-feedback approach (2), the state equation of system (1) can be reformulated in the form:

$$x(k+1) = A_{cl}x(k) + Bv(k) + D\theta(k) \tag{3}$$

where the new system matrix is given by $A_{cl} = (A - BK)$. Note that the control strategy proposed in the following sections also works without the semi-feedback approach, i.e. $u(k) = v(k)$. In this case, the proposed procedure can be used without modification and, in the case of an open-loop stable process, the stabilizing conditions (presented later in this section) are also valid.

The cost function is a quadratic performance index given by:

$$\begin{aligned} V(x, \boldsymbol{v}, \boldsymbol{\theta}) = &\sum_{j=0}^{N-1} x(k+j|k)^T Q x(k+j|k) + \sum_{j=0}^{N-1} u(k+j|k)^T R u(k+j|k) \\ &+ x(k+N|k)^T P x(k+N|k) \end{aligned} \tag{4}$$

where $x(k|k) = x$ is the current state and $x(k+j|k)$ represents the prediction of the state for $k+j$ made at k. The current input signal is $u(k|k) = -Kx(k|k) + v(k|k)$ and the future input for $k+j$ calculated at k is denoted $u(k+j|k) = -Kx(k+j|k) + v(k+j|k)$. The input correction sequence along the prediction horizon N is defined generally as $\boldsymbol{v} = [v(k|k)^T, v(k+1|k)^T, \ldots, v(k+N-1|k)^T]^T$. Analogously, the sequence of future values of the uncertainty is denoted by $\boldsymbol{\theta} = [\theta(k)^T, \ldots, \theta(k+N-1)^T]^T$ and the set of possible uncertainty trajectories is defined by $\boldsymbol{\Theta} = \{\theta \in \mathbb{R}^{N \cdot n_\theta} : ||\theta||_\infty \leq \varepsilon\}$. The matrices Q, $P \in \mathbb{R}^{n_x \times n_x}$ and $R \in \mathbb{R}^{n_u \times n_u}$ are symmetric positive definite matrices used as weighting parameters.

In MMMPC strategies [2], the input correction sequence is computed minimizing the worst case of the predicted evolution of the process state or output. The worst case cost is calculated maximizing the cost function (4) with respect to the uncertainty considered in the prediction model (3). Thus, the input correction sequence is computed solving the following min–max optimization problem:

$$\begin{aligned} &\boldsymbol{v}^* = arg \min_{v} \max_{\theta \in \Theta} V(x, \boldsymbol{v}, \boldsymbol{\theta}) \\ &\text{s.t. } F_u u(k+j|k) + F_x x(k+j|k) \leq b_c \\ &\quad j = 0, \ldots, N-1, \quad \forall \boldsymbol{\theta} \in \boldsymbol{\Theta} \\ &\quad x(k+N|k) \in \Omega, \quad \forall \boldsymbol{\theta} \in \boldsymbol{\Theta} \end{aligned} \tag{5}$$

where a terminal region constraint $x(k+N|k) \in \Omega$, with Ω being a polyhedron, has been included in order to ensure stability of the control law [16]. The terminal region Ω and the matrix P are assumed to satisfy the following conditions:

- C1: If $x \in \Omega$ then $A_{CL}x + D\theta \in \Omega$, for every $\theta \in \{\theta \in \mathbb{R}^{n_\theta} : ||\theta||_\infty \leq \varepsilon\}$.
- C2: If $x \in \Omega$ then $u(x) = -Kx + v \in U$, where $U \triangleq \{u : F_u u + F_x x \leq b_c\}$.
- C3: $P - A_{CL}^T P A_{CL} > Q + K^T R K$.

Note that the stability of A_{CL} guarantees the existence of a positive definite matrix P which satisfies condition C3.

With $x(k+j|k)$ and $u(k+j|k)$ depending linearly on x, $\mathbf{v}$ and $\boldsymbol{\theta}$, the linear constraints of problem (5) can be rewritten as [5]:

$$M_x^{[i]} x + M_v^{[i]} \boldsymbol{v} + M_\theta^{[i]} \boldsymbol{\theta} \leq b_\theta^{[i]}, \quad i = 1 \ldots, n_c, \quad \forall \boldsymbol{\theta} \in \boldsymbol{\Theta} \tag{6}$$

where $M_x^{[i]}$, $M_v^{[i]}$, $M_\theta^{[i]}$ denote the ith rows of M_x, M_v and M_θ, respectively, and $b_\theta^{[i]}$ is the ith component of $\boldsymbol{b}_\theta \in \mathbb{R}^{n_c}$. Then, taking into account that:

$$\max_{\theta \in \boldsymbol{\Theta}} M_\theta^{[i]} \boldsymbol{\theta} = \max_{||\theta||_\infty \leq \varepsilon} M_\theta^{[i]} \boldsymbol{\theta} = \varepsilon ||M_\theta^{[i]}||_1 \tag{7}$$

the robust fulfilment of the constraints is satisfied if and only if $M_x^{[i]} x + M_v^{[i]} \boldsymbol{v} + \varepsilon ||M_\theta^{[i]}||_1 \leq b_\theta^{[i]}$ for $i = 1, \ldots, n_c$ [15]. With $b_\varepsilon^{[i]} = b_\theta^{[i]} - \varepsilon ||M_\theta^{[i]}||_1$, the set of linear constraints:

$$M_x x + M_v \boldsymbol{v} \leq \boldsymbol{b}_\varepsilon \tag{8}$$

guarantees robust constraint satisfaction. Note that this is a necessary and sufficient condition.

Using the state equation (3) and the semi-feedback approach (2) in the performance index (4), the cost can be evaluated as a quadratic function:

$$\begin{aligned} V(x, \boldsymbol{v}, \boldsymbol{\theta}) = &\boldsymbol{v}^T M_{vv} \boldsymbol{v} + \boldsymbol{\theta}^T M_{\theta\theta} \boldsymbol{\theta} + 2\theta^T M_{\theta v} \boldsymbol{v} \\ &+ 2x^T M_{vf}^T \boldsymbol{v} + 2\boldsymbol{\theta}^T M_{\theta f} x + x^T M_{ff} x \end{aligned} \tag{9}$$

where the matrices can be obtained from the system and the control parameters [5]. With (9) being a convex cost function in $\boldsymbol{\theta}$, the solution to the maximization problem in (5) can be found at least in one of the vertices of $\boldsymbol{\Theta}$. Then, based on (9), the maximum cost for a given x and $\boldsymbol{v}$ is denoted as:

$$\begin{aligned} V^*(x, \boldsymbol{v}) &= \max_{\theta \in \text{vert}(\boldsymbol{\Theta})} V(x, \boldsymbol{v}, \boldsymbol{\theta}) \\ &= \max_{\theta \in \text{vert}(\boldsymbol{\Theta})} \boldsymbol{\theta}^T H \boldsymbol{\theta} + 2\boldsymbol{\theta}^T \boldsymbol{q}(x, \boldsymbol{v}) + V(x, \boldsymbol{v}, 0) \end{aligned} \tag{10}$$

where $\text{vert}(\boldsymbol{\Theta})$ denotes the set of vertices of $\boldsymbol{\Theta}$ [5] and $V(x, \boldsymbol{v}, 0)$ is the nominal cost, i.e. the part of the cost that does not depend on the uncertainty sequence $\boldsymbol{\theta}$.

With the worst case cost (10) and the robust linear constraints (8), the min–max problem (5) can be rewritten as:

$$\begin{aligned} \boldsymbol{v}^* &= arg \min_{v} V^*(x, \boldsymbol{v}) \\ \text{s.t. } & M_x x + M_v \boldsymbol{v} \leq \boldsymbol{b}_\varepsilon \end{aligned} \tag{11}$$

and the system is controlled by $u(k|k) = -Kx(k) + v^*(k|k)$. The maximization of (10) is an NP-hard optimization problem which requires the evaluation of the cost function for all vertices. With the complexity of the maximization problem (10) growing exponentially with the considered horizon, the optimization problem can only be solved in real time for short prediction horizons and small dimensions of θ.

A computationally efficient MMMPC strategy based on an upper bound of the worst case cost has been proposed in Ref. [10]. The used upper bound is the trace of a diagonal matrix which can be obtained by simple matrix operations. The matrix is computed so that the error introduced by the upper bound is minimized. The following section resumes the MMMPC strategy [10] and defines the resulting control law.

3. Min–Max MPC based on an upper bound of the worst case cost

The worst case cost $V^*(x, \boldsymbol{v})$ (10) can be represented as an augmented optimization problem in matrix form:

$$V^*(x, \boldsymbol{v}) = \max_{||z||_\infty \leq 1} z^T M(x, \boldsymbol{v}) z \tag{12}$$

with the vector $\boldsymbol{z} \in \mathbb{R}^{n_z}$ and the matrix $M(x, v) \in \mathbb{R}^{n_z \times n_z}$ given by:

$$\boldsymbol{z} = \begin{bmatrix} \frac{\theta}{\varepsilon} \\ 1 \end{bmatrix}, \quad M(x, \boldsymbol{v}) = \begin{bmatrix} \varepsilon^2 H & \varepsilon \boldsymbol{q}(x, \boldsymbol{v}) \\ \varepsilon \boldsymbol{q}(x, \boldsymbol{v})^T & V(x, \boldsymbol{v}, 0) \end{bmatrix} \tag{13}$$

and $n_z = Nn_\theta + 1$.

Consider the augmented maximization problem (12) and diagonal matrix $S \in \mathbb{R}^{n_z \times n_z}$ with the diagonal elements given by $S^{[ii]}$. For[1] $S \geq M$, the statement:

$$\boldsymbol{z}^T M \boldsymbol{z} \leq \boldsymbol{z}^T S \boldsymbol{z} = \sum_{i=1}^{n} S^{[ii]} (z^{[i]})^2 \leq \text{trace}(S) ||z||_\infty^2 \leq \text{trace}(S) \tag{14}$$

is true and, as a direct consequence, the trace of S represents an upper bound of the augmented optimization problem (12).

In order to find the smallest diagonal matrix S satisfying the inequality $S \geq M$, the diagonalization approach proposed in Ref. [10] can be used. For a given x and $\boldsymbol{v}$ the computation of the upper bound $\sigma(M) = \text{trace}(S)$ can be carried out by the following procedure:

Procedure 1. Computation of $\sigma(M)$ such that $\sigma(M) \geq \max_{||z||_\infty \leq 1} \boldsymbol{z}^T M \boldsymbol{z}$.

(1) Set $S = M \in \mathbb{R}^{n_z \times n_z}$.
(2) For $k = 1$ to $n_z - 1$.
(3) Let $M_{sub} = [S^{[ij]}]$ for $i, j = k, \ldots, n_z$.
(4) Compute $\alpha = \sqrt{||\boldsymbol{b}||_1}$ for $M_{sub} = \begin{bmatrix} a & \boldsymbol{b}^T \\ \boldsymbol{b} & M_r \end{bmatrix} \boldsymbol{z}$.
(5) Make $\varphi_e = [\alpha, (-\boldsymbol{b}^T/\alpha)]^T$.
(6) Make $\varphi_k = [0, \ldots, 0, \varphi_e^T]^T$.
(7) Diagonalize S by $S = S + \varphi_k \varphi_k^T$.
(8) Endfor.
(9) Compute the upper bound from $\sigma(M) = \sum_{i=1}^{n_z} S^{[ii]}$.

[1] In this work a matrix inequality of the type $S \geq M$ is fulfilled if and only if $S - M$ is positive semi-definite.

For a detailed description of the diagonalization given in Procedure 1 and an analysis of the suboptimality of the resulting upper bound $\sigma(M)$ the reader is referred to [10].

The diagonal matrix S computed in Procedure 1 satisfies the condition $S \geq M$ (note that only positive semi-definite matrices $\varphi_k \varphi_k^T$ have been added to S during the diagonalization process) and, as a consequence, (14) is fulfilled. Then, denoting $\hat{V}^*(x, \boldsymbol{v}) = \sigma(M) = \text{trace}(S)$ and combining (10) and (14), the following statement for the worst case cost can be made:

$$\begin{aligned} V^*(x, \boldsymbol{v}) &= \max_{||z||_\infty \leq 1} z^T \begin{bmatrix} \varepsilon^2 H & \varepsilon \boldsymbol{q}(x, v) \\ \varepsilon \boldsymbol{q}(x, \boldsymbol{v})^T & V(x, \boldsymbol{v}, 0) \end{bmatrix} z \\ &\leq \sigma \left(\begin{bmatrix} \varepsilon^2 H & \varepsilon \boldsymbol{q}(x, \boldsymbol{v}) \\ \varepsilon \boldsymbol{q}(x, v)^T & V(x, \boldsymbol{v}, 0) \end{bmatrix} \right) = \hat{V}^*(x, \boldsymbol{v}) \end{aligned} \tag{15}$$

Hence, $\sigma(M)$ calculated in Procedure 1 represents an upper bound of the worst case cost and can be used in an MMMPC strategy where the input correction sequence is the solution of the problem:

$$\begin{aligned} \hat{v}^* &= arg \min_{v} \sigma \left(\begin{bmatrix} \varepsilon^2 H & \varepsilon \boldsymbol{q}(x, \boldsymbol{v}) \\ \varepsilon \boldsymbol{q}(x, \boldsymbol{v})^T & V(x, \boldsymbol{v}, 0) \end{bmatrix} \right) \\ \text{s.t. } & M_x x + M_v \boldsymbol{v} \leq \boldsymbol{b}_\varepsilon \end{aligned} \tag{16}$$

Finally, the control law $\hat{K}_{MPC}(x(k))$ resulting from the MMMPC optimization problem can be used in a receding horizon control strategy with the input defined by $\hat{u}(k|k) = -Kx(k) + \hat{v}^*(k|k)$.

Remark. Each diagonalization step has a computational complexity of $O(n_z^2)$, leading to a computational complexity of $O(n_z^3)$ of the procedure. In contrast, the minimization of the original min–max problem (11) requires approximately 2^{n_z} operations. This means that the use of the proposed upper bound reduces considerably the number of necessary operations and allows the evaluation of the cost function in polynomial time. In fact, the diagonalization procedure can be stopped if at a certain iteration the partially diagonalized matrix S has all elements of the submatrix M_{sub} of step 3 nonnegative. In this case, the best upper bound will be the sum of the absolute values of all entries of matrix S and a further diagonalization would not improve the bound.

3.1. Choosing an initial condition

The computation of the input correction sequence $\hat{\boldsymbol{v}}^*$ (16) has to be initialized with a feasible solution to the optimization problem (11) in order to guarantee stability of the MMMPC strategy (for the stability proof see Section 4). Therefore, consider the matrix H (10) which can be used to construct a diagonal matrix T with the elements on the main diagonal defined by:

$$T^{[ii]} = \sum_{j=1}^{Nn_\theta} |H^{[ij]}| \quad \text{for } i = 1, \ldots, Nn_\theta \tag{17}$$

The off-diagonal elements are given by $T^{[ij]} = 0 \, \forall \, i \neq j$, $i = 1, \ldots, Nn_\theta$ and $j = 1, \ldots, Nn_\theta$. With the new matrix T an approximated cost function

$$\tilde{V}(x, \boldsymbol{v}, \boldsymbol{\theta}) = \boldsymbol{\theta}^T T \boldsymbol{\theta} + 2\boldsymbol{\theta}^T \boldsymbol{q}(x, \boldsymbol{v}) + V(x, \boldsymbol{v}, 0) \tag{18}$$

can be defined. With $T \geq H$ the statement

$$\tilde{V}(x, \boldsymbol{v}, \boldsymbol{\theta}) \geq V(x, \boldsymbol{v}, \boldsymbol{\theta}) \tag{19}$$

holds, i.e. $\tilde{V}(x, \boldsymbol{v}, \boldsymbol{\theta})$ represents a simple upper bound for the cost function $V(x, \boldsymbol{v}, \boldsymbol{\theta})$ given in (9). Then, the maximum of $\tilde{V}(x, \boldsymbol{v}, \boldsymbol{\theta})$, corresponding to the worst case cost of the approximated cost function, can be calculated easily by:

$$\tilde{V}^*(x, \boldsymbol{v}) = V(x, \boldsymbol{v}, 0) + \left\| H \right\|_s \varepsilon^2 + 2\varepsilon \left\| \boldsymbol{q}(x, \boldsymbol{v})^T \right\|_1 \tag{20}$$

where $\left\|H\right\|_s$ denotes the sum of the absolute values of the elements of H or, identically $\left\|H\right\|_s = \text{trace}(T)$. With the worst case cost (20) being a convex function in $\boldsymbol{v}$, the minimization problem can be solved by quadratic programming (QP). Hence, the optimal solution based on the simple upper bound of the worst case cost (20) is defined as:

$$\begin{aligned} &\tilde{v}^* = arg\min_{v} \tilde{V}^*(x, \boldsymbol{v}) \\ &\text{s.t.}\, M_x x + M_v \boldsymbol{v} \le \boldsymbol{b}_\varepsilon \end{aligned} \tag{21}$$

Finally, the solution (21) can be used as an initial feasible solution to the optimization problem (16). Note that the initial solution $\tilde{\boldsymbol{v}}^*$ has to be considered in the computation of the matrix M (13) in order to guarantee stability (see Section 4).

4. Stability of the control law

In the first place, some necessary properties to ensure the stability of the proposed control strategy will be presented. Consider the solutions $\boldsymbol{v}^*$, $\hat{\boldsymbol{v}}^*$ and $\tilde{\boldsymbol{v}}^*$ of the minimization problems (11), (16) and (21), respectively. Denote also $V^*(x) = V^*(x, \boldsymbol{v}^*)$, $\hat{V}^*(x) = \hat{V}^*(x, \hat{\boldsymbol{v}}^*)$ and $\tilde{V}^*(x) = \tilde{V}^*(x, \tilde{\boldsymbol{v}}^*)$. Note that the optimization problems (11), (16) and (21) have the same feasibility region as the constraints are the same.

Property 1. *The minimum costs $\hat{V}^*(x)$ and $\tilde{V}^*(x)$ of the optimization problems (16) and (21) satisfy:*

$$\hat{V}^*(x) \le \tilde{V}^*(x) \tag{22}$$

when $\tilde{\boldsymbol{v}}^*$ is used as initial solution to the optimization problem (16).

Proof. Taking into account the definition of $\hat{V}^*(x)$ and that $\hat{\boldsymbol{v}}^*$ is the minimizer of $\hat{V}^*(x, \boldsymbol{v})$ it is evident that

$$\hat{V}^*(x, \tilde{\boldsymbol{v}}^*) \ge \hat{V}^*(x) \tag{23}$$

Thus, in order to prove that $\hat{V}^*(x) \le \tilde{V}^*(x)$ it suffices to show that $\tilde{V}^*(x, \tilde{\boldsymbol{v}}^*) \ge \hat{V}^*(x, \tilde{\boldsymbol{v}}^*)$. First, note that taking into account that $V(x, \boldsymbol{v}, 0) \ge 0$:

$$\begin{aligned} \tilde{V}^*(x, \tilde{\boldsymbol{v}}^*) &= ||M(\tilde{\boldsymbol{v}}^*)||_1 \left\| \begin{bmatrix} \varepsilon^2 H & \varepsilon \boldsymbol{q}(x, \tilde{\boldsymbol{v}}^*) \\ \varepsilon \boldsymbol{q}(x, \tilde{\boldsymbol{v}}^*)^T & V(x, \tilde{\boldsymbol{v}}^*, 0) \end{bmatrix} \right\|_s = \left\| \begin{bmatrix} a & \boldsymbol{b}^T \\ \boldsymbol{b} & M_r \end{bmatrix} \right\|_s \\ &= a| + 2||\boldsymbol{b}||_1 + ||M_r||_s \end{aligned} \tag{24}$$

On the other hand $\hat{V}^*(x, \tilde{v}^*)$ is equal to trace(S), that is the sum of the elements of the diagonal matrix computed in Procedure 1 which also is equal to $||S||_s$ as $S \ge 0$. The initial value of S is $S = M(\tilde{\boldsymbol{v}}^*)$, thus the sum of the absolute values of S is equal to $\tilde{V}^*(x, \tilde{\boldsymbol{v}}^*)$. Taking into account the definition $\alpha = \sqrt{||\boldsymbol{b}||_1}$ (see Procedure 1), $||S||_s$ after the first diagonalization step becomes:

$$\left\| \begin{matrix} a + ||\boldsymbol{b}||_1 & 0 \\ 0 & M_r + \dfrac{\boldsymbol{b}\boldsymbol{b}^T}{||\boldsymbol{b}||_1} \end{matrix} \right\|_s \le |a| + ||\boldsymbol{b}||_1 + ||M_r||_s + \left\| \frac{\boldsymbol{b}\boldsymbol{b}^T}{||\boldsymbol{b}||_1} \right\|_1 \tag{25}$$

Taking into account that $\left\| \frac{\boldsymbol{b}\boldsymbol{b}^T}{||\boldsymbol{b}||_1} \right\|_1 = ||\boldsymbol{b}||_1$ it follows that:

$$\left\| \begin{matrix} a + ||\boldsymbol{b}||_1 & 0 \\ 0 & M_r + \dfrac{\boldsymbol{b}\boldsymbol{b}^T}{||\boldsymbol{b}||_s} \end{matrix} \right\|_1 \le ||M(\tilde{\boldsymbol{v}}^*)||_s \tag{26}$$

and thus every diagonalization step decreases $||S||_s$. This proves that:

$$\hat{V}^*(x, \tilde{\boldsymbol{v}}^*) \le \tilde{V}^*(x, \tilde{\boldsymbol{v}}^*) \tag{27}$$

and this completes the proof. □

It is clear that the optimal solution $\hat{\boldsymbol{v}}^*$ of problem (16) is a suboptimal feasible solution for problem (11). As it is claimed in the following property, the difference between the optimal value of the original objective function and the value obtained with $\hat{\boldsymbol{v}}^*$ is bounded by trace(T)ε^2.

Property 2. *It holds that:*

$$V^*(x, \hat{\boldsymbol{v}}^*) - \text{trace}(T)\varepsilon^2 \le V^*(x) \tag{28}$$

Proof. Note that $V^*(x) = V^*(x, \boldsymbol{v}^*)$. On the other hand:

$$\tilde{V}(x, \boldsymbol{v}, \boldsymbol{\theta}) = V(x, \boldsymbol{v}, \boldsymbol{\theta}) + \boldsymbol{\theta}^T (T - H)\boldsymbol{\theta}. \tag{29}$$

Taking into account that $T \ge H \ge 0$, $||\boldsymbol{\theta}||_\infty \le \varepsilon$ and that T is a diagonal matrix, the statement:

$$\tilde{V}(x, \boldsymbol{v}, \boldsymbol{\theta}) \le V(x, \boldsymbol{v}, \boldsymbol{\theta}) + \boldsymbol{\theta}^T T \boldsymbol{\theta} \le V(x, \boldsymbol{v}, \boldsymbol{\theta}) + \text{trace}(T)\varepsilon^2 \tag{30}$$

is true. From (30) it can be inferred that:

$$V^*(x, \boldsymbol{v}^*) \ge \tilde{V}^*(x, \boldsymbol{v}^*) - \text{trace}(T)\varepsilon^2 \tag{31}$$

Then, with $\tilde{\boldsymbol{v}}^*$ being the minimizer of $\tilde{V}^*(x, \boldsymbol{v})$ and $V^*(x) = V^*(x, \boldsymbol{v}^*)$, (31) can be rewritten as:

$$V^*(x) \ge \tilde{V}^*(x) - \text{trace}(T)\varepsilon^2 \tag{32}$$

Now, from the relation $\hat{V}^*(x) \le \tilde{V}^*(x)$ (see Property 1) and (32) follows that:

$$V^*(x) \ge \hat{V}^*(x) - \text{trace}(T)\varepsilon^2 \tag{33}$$

Finally, with the upper bound $\hat{V}^*(x, \boldsymbol{v}) \ge V^*(x, \boldsymbol{v})$ and (33), the statement for the optimal cost:

$$V^*(x) \ge V^*(x, \hat{\boldsymbol{v}}^*) - \text{trace}(T)\varepsilon^2 \tag{34}$$

is satisfied. This completes the proof. □

The following property, which is proven in [17] will be used in the proof of the stability of the proposed approach (see Theorem 1 below).

Property 3. *Consider that assumptions C1, C2 and C3 are satisfied. Furthermore, let $\boldsymbol{v} = [v(k|k), v(k+1|k), \ldots, v(k+N-1|k)]^T$ and $\boldsymbol{v}_s$ a shifted version of $\mathbf{v}$ computed as $\boldsymbol{v}_s = [v(k+1|k), v(k+2|k), \ldots, v(k+N-1|k), 0]^T$. If $\mathbf{v}$ is feasible for problem (11) at $x(k)$, then $\boldsymbol{v}_s$ is also feasible at $x(k+1)$ and there is a $\gamma > 0$ such that for every feasible sequence $\mathbf{v}$:*

$$V^*(x(k+1), \boldsymbol{v}_s) \le V^*(x(k), \boldsymbol{v}) - x(k)^T Q x(k) + \gamma\varepsilon^2 \tag{35}$$

Proof. See [17] for a proof. □

Theorem 1. *Under the assumption that the conditions C1, C2 and C3 are satisfied, the control law $\hat{K}_{MPC}(x(k))$ given by $\hat{u}(k|k) = -Kx(k) + \hat{\boldsymbol{v}}^*(k|k)$ stabilizes system (1).*

Proof. Consider the input sequence $\hat{\boldsymbol{v}}_s^*$ being a shifted version (as in Property 3) of $\hat{\boldsymbol{v}}^*$. Due to non-optimality of $\hat{\boldsymbol{v}}_s^*$ for problem (11) it holds that

$$V^*(x(k+1)) \le V^*(x(k+1), \hat{\boldsymbol{v}}_s^*) \tag{36}$$

Note that $\hat{\boldsymbol{v}}_s^*$ is feasible for both (16) and (11), thus by Property 3:

$$V^*(x(k+1), \hat{\boldsymbol{v}}_s^*) \le V^*(x(k), \hat{\boldsymbol{v}}^*) - x(k)^T Q x(k) + \gamma\varepsilon^2 \tag{37}$$

Now, taking in account $V^*(x(k), \hat{\boldsymbol{v}}^*) \le V^*(x(k)) + \text{trace}(T)\varepsilon^2$ (see Property 2) and using (36) and (37) can be rewritten in the form:

$$V^*(x(k+1)) - V^*(x(k)) \le -x(k)^T Q x(k) + (\gamma + \text{trace}(T))\varepsilon^2 \tag{38}$$

and leads to the set:

$$\Phi_\varepsilon = \{x \in \mathbb{R}^n : (11) \text{ is feasible and } x(k)^T Q x(k) \le (\gamma + \text{trace}(T))\varepsilon^2\} \tag{39}$$

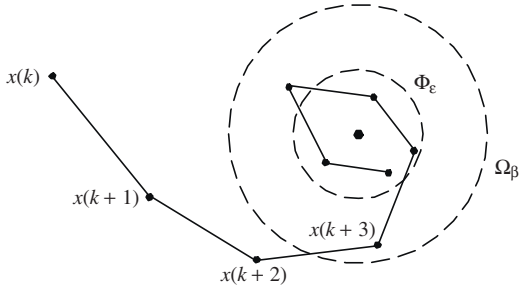

Fig. 1. Evolution of the system state $x(\cdot)$ and the sets Ω_β and Φ_ε.

containing the origin. As a consequence, the system state is steered into Φ_ε from any arbitrary $x(k)$. After entering the set Φ_ε the state can remain inside or leave the set as it is not guaranteed that the optimal worst case cost decreases within the set Φ_ε. Under consideration of $-x(k)^T Q x(k) \leq 0$ and (38), the cost in $k+1$ satisfies:

$$V^*(x(k+1)) \leq V^*(x(k)) + (\gamma + \text{trace}(T))\varepsilon^2 \tag{40}$$

Now, for every $x(k) \in \Phi_\varepsilon$ holds:

$$V(x(k)) + (\gamma + \text{trace}(T))\varepsilon^2 \leq \max_{x \in \Phi_\varepsilon} V(x) + (\gamma + \text{trace}(T)) = \beta \tag{41}$$

It is clear from (40) and (41) that for every $x(k) \in \Phi_\varepsilon$ the cost in $k+1$ satisfies:

$$V(x^*(k+1)) \leq \beta \tag{42}$$

As a consequence, whenever the state enters the set Φ_ε the system will evolve into the set:

$$\Omega_\beta = \left\{ x \in \mathbb{R}^n : V^*(x) \leq \beta \right\} \tag{43}$$

Although the state can leave the set Φ_ε, it will remain inside the set Ω_β. With the state being in Ω_β, the system is steered again and again into Φ_ε (see Fig. 1). Hence, the state is ultimately bounded and the system is input-to-state practical stable using the control law $\hat{K}_{MPC}(x(k))$ given by $\hat{u}(k|k) = -Kx(k) + \hat{v}^*(k|k)$. □

5. Process description

A real process represented by a pilot plant has been chosen for the application of the proposed algorithm. The process has been studied previously by several authors [18,19] and has been used as a benchmark for control purposes [20].

5.1. Laboratory process

The pilot plant shown in Fig. 2 is used to emulate a continuous stirred tank reactor (CSTR) based on temperature changes as done in Ref. [21]. The main elements of the system are the tank reactor, an electric resistance, a cooling jacket, a valve to manipulate the flow rate through the cooling jacket as well as a water tank. The general plant structure with the mentioned elements is given in the schematic diagram in Fig. 3.

The cooling jacket is used to reduce the caloric energy of the reactor content. The heat dissipation can be regulated by the valve v_8 manipulating the flow rate F_j through the cooling jacket. The cooling fluid, water, circulating through the cooling jacket is taken from a tank with a capacity of 1 m^3. After circulating through the jacket the cooling fluid returns to the tank. To maintain the temperature of the cold water constant, the tank has an auxiliary cooler controlled by a thermostat which maintains the temperature T_{T2} near to a desired value in an interval of approximately 1°.

The reactant is supplied to the reactor by the feed $F_{f,in}$ to keep the chemical reaction active. Before entering the reactor, the feed

Fig. 2. Continuous stirred tank reactor used to apply the MMMPC based on an upper bound of the worst case cost.

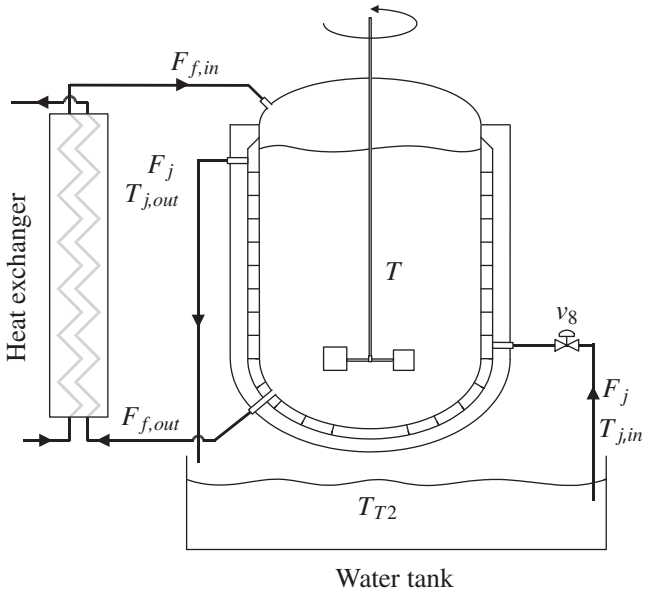

Fig. 3. Diagram of the CSTR emulated by the pilot plant showing the emulated feed $F_{f,in}$ and outflow $F_{f,out}$.

Table 1
Model parameters and constant variables of the chemical reaction.

Parameter	Value	Unit
k_0	1.2650×10^{17}	1/mol s
C_p	4.18	J/K kg
ΔH	−105.57	kJ/mol
E/R	13,550	K
Variable	Value	Unit
M	25	kg
$C_{A,in}$	1.2	mol/l
F_f	0.05	1/s
$T_{j,in}$	291.15	K

passes through a heat exchanger in order to reduce the temperature difference between the feed and the reactor content. The outflow $F_{f,out}$ is used to keep the volume of the reactor content constant. As a consequence, as feed and outflow have the same flow rate and nearly the same temperature, the two flows hardly provoke temperature changes in the interior of the reactor.

To emulate exothermic reactions, the reactor possesses an electric resistance in order to supply caloric energy. The energy to be supplied by the 14.4 kW electric resistance is calculated with a mathematical model of the reaction (see Section 5.2). The use of a resistance has the practical advantage that no chemical reaction takes place in the reactor, instead the reaction is emulated on basis of temperature changes, as done in Ref. [21].

5.2. Mathematical model

Although it is not necessary to have a mathematical model for the design of the min–max predictive controller, this section shows the process model to emphasize its nonlinear character. The mathematical model also justifies the way to emulate the heat generated by the chemical reaction with the aid of the resistance.

The emulated chemical reaction, representing a refinement process, was used previously in Ref. [22,14,15]. Considering identical flow rates for the feed and the outflow, i.e. $F_f = F_{f,in} = F_{f,out}$, the reactor volume V and the mass M are constant. The temperature changes of the reactor content can be defined as:

$$\frac{dT}{dt} = -\frac{F_j}{V}(T_{j,out} - T_{j,in}) + \frac{(-\Delta H)\cdot V}{MC_p} k_0 e^{-E/(RT)} C_A^2 \tag{44}$$

where the first term considers the heat dissipation by the cooling jacket and the second term denotes the generated heat by the exothermic chemical reaction. Note that the second term is used to calculate the heat to be supplied by the electric resistance in the reactor tank in order to emulate the chemical reaction based on temperature changes. The variables F_j, $T_{j,in}$ and $T_{j,out}$ represent the flow rate through the cooling jacket and the temperature of the cooling fluid entering and leaving the cooling jacket, respectively. C_A is the concentration of the reactant in the reactor content. It has been assumed that the feed neither supplies nor removes caloric energy from the reactor as the feed passes through a heat exchanger and enters the reactor nearly with the temperature of the reactor content.

The reactant concentration C_A in the plant reactor is calculated by:

$$\frac{dC_A}{dt} = \frac{F_f}{V}(C_{A,in} - C_A) - k_0 e^{-E/(RT)} C_A^2 \tag{45}$$

where the first term represents changes in the reactant concentration due to the feed and the outflow. The second term considers the reduction of the concentration as a result of the reactant consumption by the chemical reaction. $C_{A,in}$ denotes the reactant concentration in the feed. The model parameters and the variables used with constant values are shown in Table 1.

The chemical reaction is nonlinear in the dynamics of the temperature and the concentration due to the exponential function and the quadratic terms of the concentration in the model equations (44) and (45). Furthermore, the relation between the opening of the valve v_8 and the flow rate F_j through the cooling jacket adds some static nonlinearity to the model.

5.3. Description of the control system

The sensors and actuators of the plant are connected to a Schneider M340 programmable automation controller (PAC). The M340 is connected by Ethernet to a personal computer that runs a Vijeo Citect SCADA together with an Unity Pro software package. The proposed control algorithm has been implemented directly in Matlab/Simulink and the communication with the SCADA is done using the OPC protocol (OLE for Process Control). Hence, both the SCADA and the controller implemented in Matlab/Simulink run on the same personal computer based on a Pentium 4 processor with 3 GHz using Windows XP as operating system.

6. Experimental results

The strategy described in Section 3 has been applied to the chemical reaction process described in Section 5. In this section the experimental results will be exposed and discussed. An input–output model with integrated bounded additive uncertainty has been used in the experiments:

$$A(z^{-1})y(k) = z^{-d}B(z^{-1})u(k-1) + \frac{\theta(k)}{\Delta} \tag{46}$$

with $\Delta = 1 - z^{-1}$, $\theta(k) \in \{\theta \in \mathbb{R}^{d_y} : ||\theta||_\infty \leq \varepsilon\}$, and d_y the dimension of $y(k)$. The use of this type of prediction models results in a control law without error in steady state. The main difference between using the algorithm of Section 3 for a state space model and the given input–output model with bounded additive uncertainties is the method used to find the matrices of the cost function (9) [5]. Besides that, the algorithm can be applied as described in Section 3.

In the following section the identification of a suitable prediction model will be presented. Afterwards, the experimental results obtained from the CSTR controlled by the presented MMMPC strategy will be exposed.

6.1. Identification of the prediction model

A Pseudo-Random Multilevel Step Sequence (PRMSS) has been applied to the recirculation valve with the objective of collecting data for the parameter identification of the prediction model. The periods of the PRMSS have been chosen sufficiently long to observe the reaction of the pilot plant to changes in the input (see Fig. 4). It can be observed that the input–output gain is negative and clearly variable (greater gain for low openings of v_8). A first order transfer function model with delay is proposed as prediction model. It has to be mentioned that the proposed low order prediction model cannot describe correctly the nonlinear dynamic behavior of the used process. Therefore, the used process is a good candidate to be controlled by a control strategy considering uncertainties and disturbances.

Using the data of Fig. 4 the system delay was approximated with $t_d = 31.25$ s. Taking in account the response time of the system, the sampling period has been chosen to $T_s = 60$ s. The delay of the system was rounded to 1 sampling time in order to avoid approximations of the time delay, e.g. Padé approximation. With the experimental data (see Fig. 4) a least squares identification has

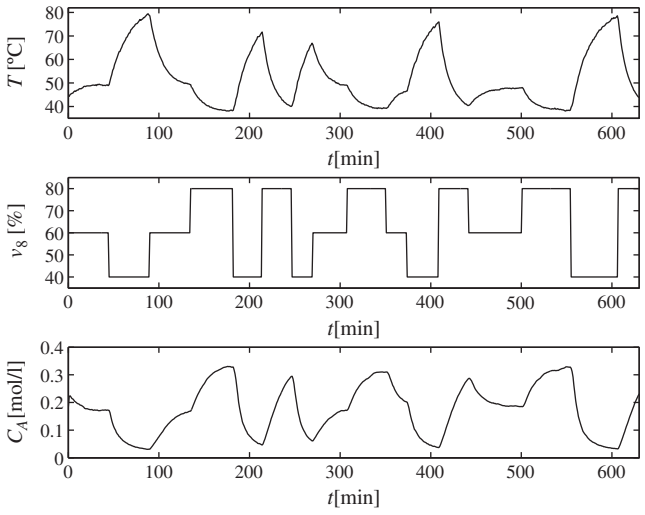

Fig. 4. Experiment for the model identification. From top to bottom: Tank temperature (T), valve opening (v_8) and reactant concentration (C_A).

been carried out and the following model has been identified:

$$y(k) = 0.941y(k-1) - 0.061u(k-2) \tag{47}$$

Thereby, the following input–output prediction model with integrated bounded additive uncertainty was obtained:

$$y(k+1|k) = 0.941y(k) - 0.061u(k-1) + \frac{\theta(k)}{\Delta} \tag{48}$$

Based upon the one step ahead prediction error (see Fig. 5) the parameter ε has been chosen to $\varepsilon = 0.4$. As a result, in 94% of the samples the one step ahead prediction error is bounded by the chosen value. In order to verify the goodness of fit of the identified model a second set of experimental data has been used to calculate the one step ahead prediction error. Fig. 6 shows the tank temperature and the one step ahead prediction error of the prediction model (48). It can be seen from the figure that the one step ahead prediction error is bounded by $\varepsilon = 0.4$ nearly throughout the whole experiment, only in a few samples the prediction error exceeds the bound. Therefore, the verification confirms the election of $\varepsilon = 0.4$ as a valid choice.

Note that in long term plant operation the parameter ε can be adjusted if necessary together with the nominal model. Furthermore, if the plant works only around an operating point or around a small interval of operating points, a less conservative upper bound of the uncertainty, i.e. a reduced value for the parameter ε, can be used.

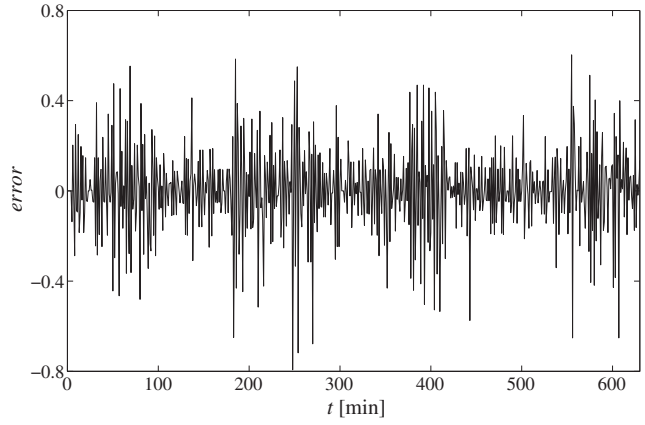

Fig. 5. One step ahead prediction error during the experiment for the model identification.

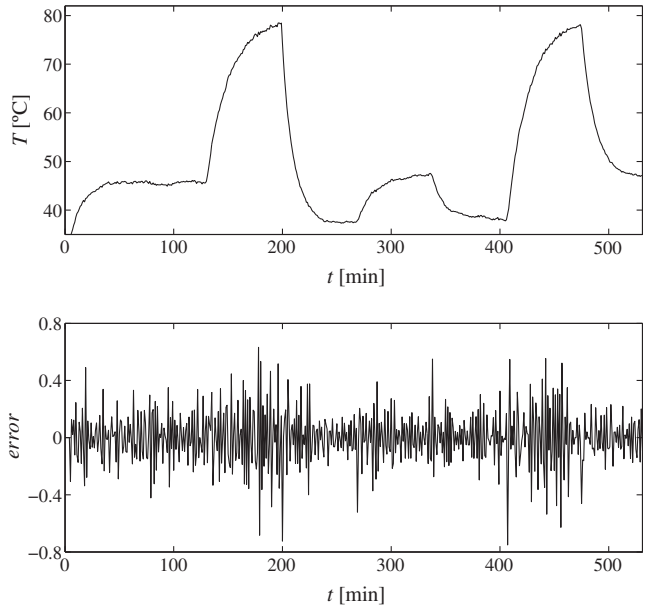

Fig. 6. Experiment to verify the goodness of fit of the prediction model (48). From top to bottom: Tank temperature (T), one step ahead prediction error.

6.2. Experimental results of the controller

The proposed control strategy was applied to the pilot plant described in Section 5.1 using (48) as a prediction model. For the implementation of the MMMPC a prediction horizon of $N = 25$, a control horizon of $N_u = 15$ and a weighting factor for the control effort of $R = 5$ were used. The choice of the prediction horizon is based on the common rule of including 1.5 times the dominant time constant of the considered process. The control horizon has been chosen to include one time constant of the process. These choices offer the possibility to show how the proposed MMMPC can be applied in real time to a broad class of processes even for large control and prediction horizons. Naturally, the system can be controlled with shorter horizons, but the high values of N and N_u emphasize that the proposed control strategy has a very low computational burden compared to that of a conventional MMMPC controller[2] and can be used in real time applications. Note that the use of different prediction and control horizons ($N \neq N_u$) in the cost function (4) requires minor changes in the matrices M_{vv}, $M_{\theta v}$ and M_{vf} in the quadratic cost function (9) as well as in the matrix G_v in the considered min–max problem (11).[3] In the implementation of the proposed control strategy the terminal constraint and the terminal cost have not been considered. With a prediction horizon of $N = 25$, including approximately 1.5 times the dominant time constant of the process, the terminal constraint is not active for the region of interest. Also, the prediction horizon is sufficiently large and therefore, the effect of not including a terminal cost can be neglected. For a formal study when it is possible to disregard the terminal constraint and terminal cost see [23–25].

Due to the varying delay of the real process a correction in the prediction of $y(k+1)$ has been used. With the Smith like predictor the predicted output at time $k+1$ using the nominal model, $\hat{y}_n(k+$

[2] In fact, a conventional MMMPC controller with such horizons could not be implemented on the pilot plant using the hardware described in Section 5.3.

[3] Defining the variable $\pi = N - N_u$ (the difference of the two horizons), the necessary adjustment of the matrices M_{vf}, G_v, $M_{\theta v}$ and M_{vv} due to different prediction and control horizons leads to the elimination of the last π rows of M_{vf}, the last π columns of G_v and $M_{\theta v}$ and the last π rows and columns of M_{vv}.

$1|k)$, is corrected as:

$$\hat{y}(k+1|k) = \hat{y}_n(k+1|k) + (\hat{y}_n(k|k) - y(k)) \tag{49}$$

being $y(k)$ the real process output at instant k. The use of a Smith like predictor is a proven approach to deal with varying and uncertain system delays (also in the field of nominal MPC [26]) which has the additional benefit of not increasing the complexity of the MPC algorithm. It has to be emphasized that MMMPC algorithms inherit the sensitiveness to uncertain and varying system delays [5] from conventional MPC controllers (although using a worst case design based on global uncertainties does help to some extent). Thus, the inclusion of a correction of the prediction by means of a Smith like predictor will help to reduce the effect of the uncertain and varying system delay. Also, this correction will improve the robustness of the controller as it is known that it can cope with other modeling errors. However, in this case, the consideration of a worst case design through a min–max formulation is responsible for much of the improvements in robustness. This can be seen later in this section in the comparisons with a nominal constrained MPC which also uses the Smith predictor correction.

In order to restrict the system input and output in the experiments, the following constraints have been used:

$$\begin{aligned} &30 \le \hat{y}(k+j|k) \le 70, \quad k = 2, \ldots, 26, \ \forall \boldsymbol{\theta} \in \mathrm{vert}(\boldsymbol{\Theta}) \\ &5 \le k+j|k) \le 100, \quad k = 0, \ldots, 14 \\ &-20 \le \Delta u(k+j|k) \le 20, \quad k = 0, \ldots, 14 \end{aligned} \tag{50}$$

The output constraints[4] are based on the physical limits of the pilot plant and include the temperature interval covered by the data sets used in the identification and validation of the prediction model (note that the upper limit of 70 °C has been chosen to avoid that the system reaches the permitted maximum temperature of the plant of 80 °C at which the pilot plant is automatically switched off). The constraints in the control signal represent the physical limits of the used valve which manipulates the flow through the cooling jacket (in fact, the valve can be closed completely, i.e. it can adopt a value of 0%, but for values below 5% the pump is automatically switched off leading to a zero flow like that of a completely closed valve). Finally, the constraints in the increments of the control signal have been chosen to avoid a too aggressive control that could move the system too fast and far away from the operating points considered during the identification process (in which the maximum step size in the input signal was about 20%).

In order to analyze the closed-loop behavior of the system controlled by the proposed MMMPC strategy, several experiments including reference tracking and disturbance rejection have been carried out. In the first place, a setpoint tracking experiment with the presented min–max control strategy was carried out (see Fig. 7). Starting in steady state with a reference of 55 °C, the setpoint is changed in $t = 30$ min to 65 °C and in $t = 90$ min to 45 °C. It can be observed in the experimental results that the min–max control strategy applies the new setpoint changes rapidly to the system and stabilizes the temperature in the setpoint in less than 20 min after the application of the changes in the reference. After the first setpoint change no overshoot can be observed whereas a marginal overshoot (approximately −0.7°C) appears after the second setpoint change. After reaching steady state the control signal shows only small variations without periodic oscillations and the concentration C_A remains in a constant level.

In the second place a setpoint tracking experiment with an error in the model of the exothermic reaction was carried out. It has to be emphasized that the heat generated by the exothermic chemical reaction is emulated by means of an electric resistance. This approach allows a simple modification of the emulated chemical reaction by changing parameters of the model (44) and (45) that it is used to compute the duty cycle of the electric resistance. The error introduced in the activation energy E of the emulated chemical reaction was held constant during the entire experiment. Due to the strong influence of the parameter E on the dynamics of the system, the mentioned parameter was increased only by 3% of the original value. The experimental results in Fig. 8 show that the control strategy stabilizes the system output in the desired reference

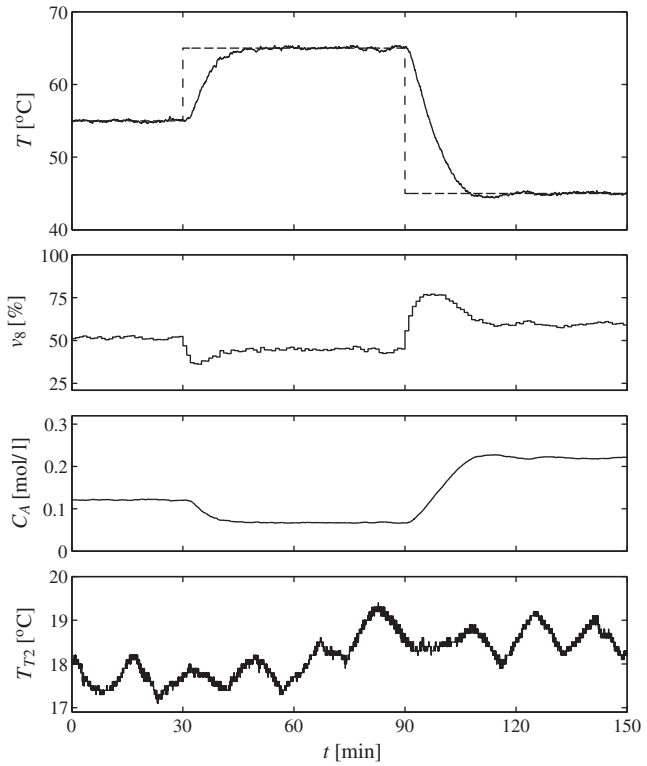

Fig. 7. Reference tracking experiment. From top to bottom: Tank temperature (T), valve opening (v_8), reactant concentration (C_A) and cold water temperature (T_{T2}).

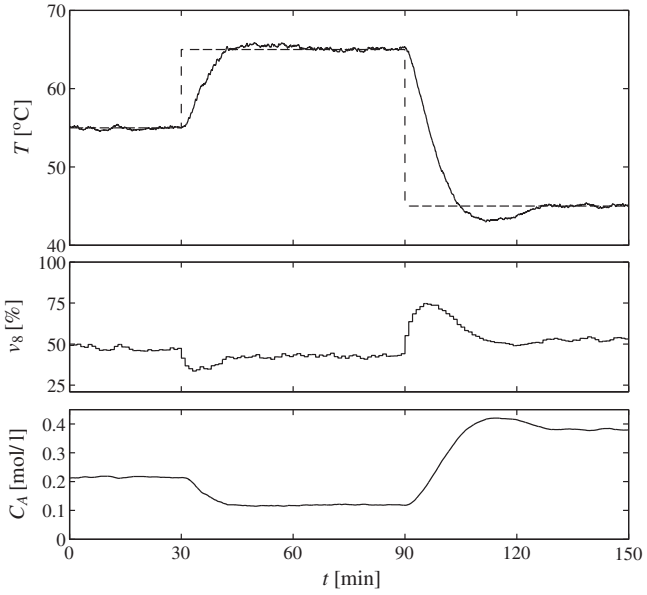

Fig. 8. Reference tracking experiment with a persistent disturbance in the emulated chemical reaction. From top to bottom: Tank temperature (T), valve opening (v_8) and reactant concentration (C_A).

[4] Note that in the output constraints the effect of the uncertainty has to be considered.

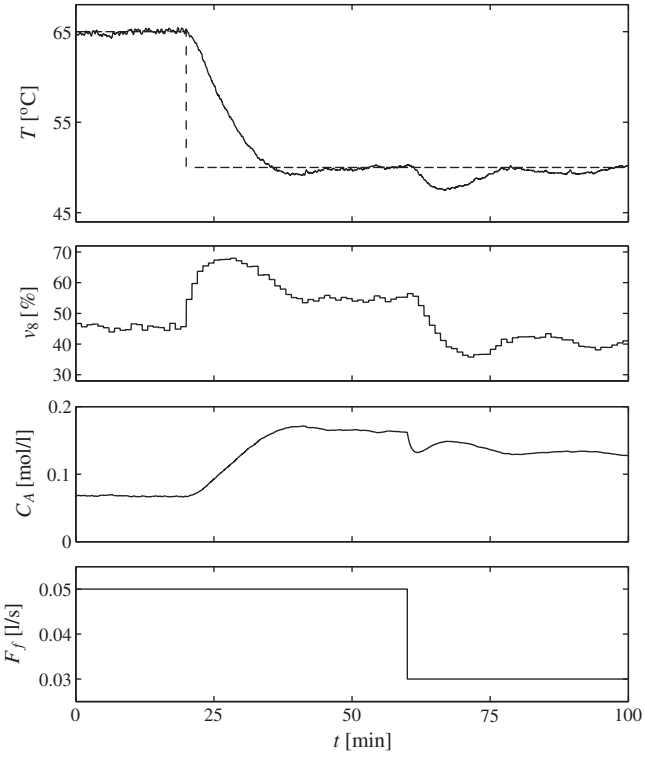

Fig. 9. Disturbance rejection experiment with a disturbance in the feed F_f. From top to bottom: Tank temperature (T), valve opening (v_8), reactant concentration (C_A) and feed (F_f).

without difficulties. Nevertheless, as a result of the model mismatch, some overshoot can be observed after the setpoint changes (approximately 0.9 °C and −2°C after the first and the second step, respectively). Comparing the results of Figs. 7 and 8 it is evident that the observed overshoot is mainly a result of the introduced model mismatch. However, the min–max control strategy shows its capability to stabilize the system in presence of a model uncertainty.

In the last experiment (see Fig. 9) with the pilot plant the disturbance rejection capabilities of the min–max control strategy were tested by means of a disturbance in the feed F_f. Starting the experiment with the nominal feed $F_f = 0.05$ l/s, the disturbance $\Delta F_f = -0.02$ l/s was applied to the system in $t = 60$ min. After the application of the disturbance it can be observed that the concentration C_A decreases and, as a consequence, the temperature falls below the given setpoint and reaches a maximum divergence of −2.5 °C. With an increasing error in the system output, the min–max control strategy partially closes the valve v_8 and compensates the effect of the reduced feed. The control strategy rejects the disturbance in approximately 20 min, but shows afterwards small oscillations in the temperature and the valve opening, totally justified by the magnitude of the disturbance (ΔF_f corresponds to an error of −40% with respect to the nominal feed).

Finally, some of the experiments carried out with the MMMPC were repeated with a constrained Generalized Predictive Control (GPC) strategy in order to compare the performance of a standard linear MPC with the one of the MMMPC strategy. A fair comparison between the two predictive controllers can only be carried out when the cost functions are the same or at least close to be equal. Therefore, the GPC was implemented with the same linear prediction model (48) and adjusted with the same tuning parameters (prediction horizon $N = 25$, control horizon $N_u = 15$ and weighting factor for the control effort $R = 5$) with exception of the uncertainty bounds that are not present in the GPC. As a result, the cost function to be minimized by the GPC is as similar as possible to the one of the MMMPC. Furthermore, the predicted output was corrected by the same Smith like predictor (49) used before in combination with the MMMPC and the same constraints (50) as in the case of the MMMPC were considered.

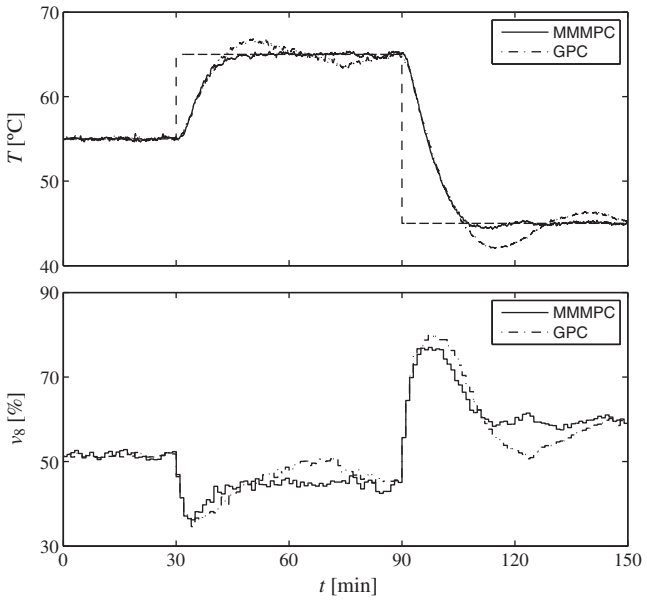

Fig. 10. Reference tracking experiments of the MMMPC (solid line) and the GPC (dash-dotted line). From top to bottom: Tank temperature (T) and valve opening (v_8).

The results obtained in a setpoint tracking experiment with the GPC (see Fig. 10) show significant oscillations both in the measured output and the computed input signal after the applied setpoint changes. Moreover, a considerable overshoot in the controlled temperature can be observed. Furthermore, a disturbance rejection experiment with a disturbance in the feed F_f was carried out with the GPC (see Fig. 11). It can be observed that the GPC shows a slow reaction to the disturbance applied in $t = 80$ min and needs approximately 30 min to compensate the output error. The direct

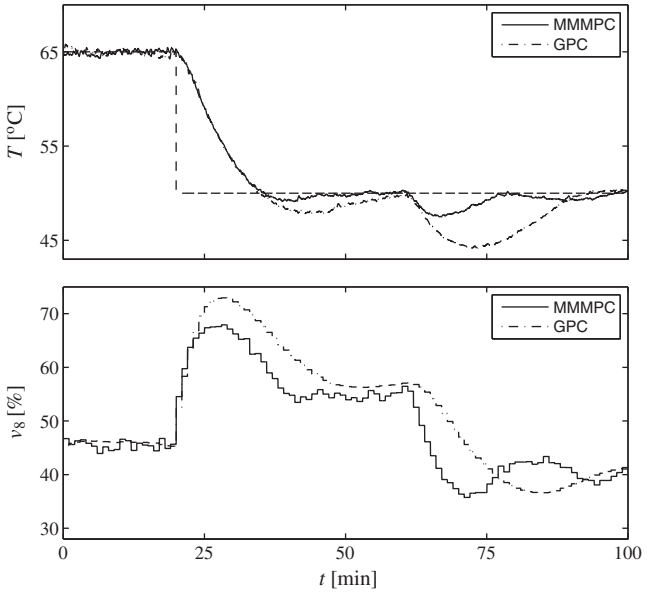

Fig. 11. Disturbance rejection experiment with a disturbance in the feed F_f with the MMMPC (solid line) and the GPC (dash-dotted line). From top to bottom: Tank temperature (T) and valve opening (v_8).

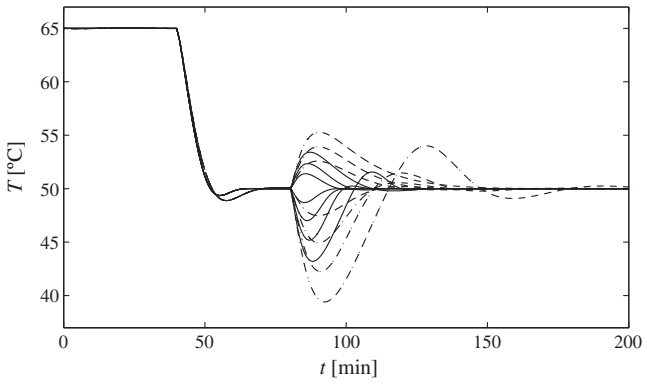

Fig. 12. Simulation results for different disturbances in the feed F_f with the MMMPC (solid line) and the GPC (dash-dotted line). Comparison of the tank temperature for the feeds $F_f = \{0.1, 0.2, 0.3, 0.4, 0.6, 0.65, 0.7\}$ l/s applied after $t = 80$ min.

Table 2
Maximum, minimum and average computation times of the MMMPC and GPC to calculate the input sequence in the presented experiments.

Strategy	$t_c^{\min}$ (s)	$t_c^{\max}$ (s)	t_c^{avg} (s)
MMMPC	0.397	3.277	0.772
GPC	0.021	0.112	0.031

comparison of the results obtained with the MMMPC and the GPC (see Figs. 10 and 11) shows the generally better performance of the MMMPC with a more efficient stabilization in the setpoint and less oscillations in the system input and output. Furthermore, the MMMPC reacts faster to the applied disturbance and compensates the resulting output error more efficiently. Although both controllers are based on the same linear prediction model, the explicit consideration of an additive uncertainty in the MMMPC strategy leads to better results and a more robust control behavior. This more robust behavior is further illustrated in Fig. 12. This figure shows the simulated[5] responses of each controller for different values of the feed F_f. It can be seen that the envelope that comprises all the responses of the MMMPC is tighter than that of the GPC, which implies a more robust behavior of the MMMPC.

The MMMPC strategy showed in the presented experiments a good behavior, both for setpoint tracking and disturbance rejection. The minimum, maximum and average computation times of the MMMPC to calculate the input sequence in the presented experiments are given in Table 2. The necessary time to compute a new input sequence is quite low (taking into account the large prediction horizon of $N = 25$) and lies clearly inside the used sampling time of $t_s = 60$ s. For comparison purposes, Table 2 also shows the computation times of the GPC. Obviously, the GPC solves the constrained optimization problem in less time than the MMMPC, but will not have the benefits of a worst case cost design. Finally, it is important to underline that the original maximization problem would require a number of operations that is proportional to 2^{Nn_θ} for each evaluation of the cost function and could not be solved within the used sampling time.

7. Conclusions

In this paper an MMMPC strategy, originally proposed in Ref. [10], has been considered. The control strategy considerably reduces the computational complexity as the maximization problem, normally carried out by the evaluation of all 2^{Nn_θ} possible vertices of the disturbance, is replaced by an algorithm of polynomial complexity. New conditions necessary to guarantee the input-to-state practical stability of the closed loop system have been presented. The control strategy has been successfully applied to a continuous stirred tank reactor.

The obtained results underlined the capability of the MMMPC strategy to stabilize the benchmark system even in presence of strong disturbances. Furthermore, some of the results of the MMMPC strategy were compared to the ones obtained with a standard GPC. The comparison of the results showed that the MMMPC strategy leads to better results in the presence of modeling errors. These experimental results together with the stability guarantee suggest that the proposed MMMPC is a valid alternative to control uncertain processes. Also the reduced computational complexity allows the use of realistic prediction and control horizons.

[5] Simulation is used in this case to ensure that all conditions are exactly the same in each experiment. Nevertheless it is noteworthy that the simulation results are congruent with the experimental results shown in Fig. 11.

Acknowledgement

Financial support by the Spanish Ministry of Education and Science under Grants DPI2007-66718-C04-01 and DPI2008-05818 is gratefully appreciated.

References

[1] H.S. Witsenhausen, A min–max control problem for sampled linear systems, IEEE Transations on Automatic Control 13 (1) (1968) 5–21.
[2] P.J. Campo, M. Morari, Robust Model Predictive Control, in: Proceedings of the 1987 American Control Conference, Minneapolis, MN, 1987, pp. 1021–1026.
[3] J.H. Lee, Z. Yu, Worst-case formulations of Model Predictive Control for systems with bounded parameters, Automatica 33 (5) (1997) 763–781.
[4] P.O.M. Scokaert, D.Q. Mayne, Min–max feedback Model Predictive Control for constrained linear systems, IEEE Transactions on Automatic Control 43 (8) (1998) 1136–1142.
[5] E.F. Camacho, C. Bordons, Model Predictive Control, 2nd ed., Springer, 2004.
[6] A. Bemporad, F. Borrelli, M. Morari, Min–max control of constrained uncertain discrete-time linear systems, IEEE Transactions on Automatic Control 48 (9) (2003) 1600–1606.
[7] E.C. Kerrigan, J.M. Maciejowski, Feedback Min–Max Model Predictive Control using a single linear program: robust stability and the explicit solution, International Journal of Robust and Nonlinear Control 14 (4) (2004) 395–413.
[8] D.R. Ramirez, E.F. Camacho, Piecewise affinity of Min–Max MPC with bounded additive uncertainties and a quadratic criterion, Automatica 42 (2) (2006) 295–302.
[9] D. Muñoz de la Peña, D.R. Ramirez, E.F. Camacho, T. Alamo, Explicit solution of Min–Max MPC with additive uncertainties and quadratic criterion, Systems and Control Letters 55 (4) (2006) 266–274.
[10] D.R. Ramirez, T. Alamo, E.F.D. Camacho, D. Muñoz de la Peña, Min–Max MPC based on a computationally efficient upper-bound of the worst case cost, Journal of Process Control 16 (5) (2006) 511–519.
[11] M.V. Kothare, V. Balakrishnan, M. Morari, Robust constrained Model Predictive Control using linear model inequalities, Automatica 32 (10) (1996) 1361–1379.
[12] Y. Lu, Y. Arkun, Quasi-Min–Max MPC algorithms for LPV systems, Automatica 36 (4) (2000) 527–540.
[13] J.A. Rossiter, Model-Based Predictive Control: A Practical Approach, CRC Press, 2003.
[14] J.K. Gruber, C. Bordons, R. Bars, R. Haber, Nonlinear predictive control of smooth nonlinear systems based on Volterra models. Application to a pilot plant, International Journal of Robust and Nonlinear Control 20 (16) (2010) 1817–1835.
[15] J.K. Gruber, D.R. Ramirez, T. Alamo, C. Bordons, E.F. Camacho, Control of a pilot plant using QP based min–max predictive control, Control Engineering Practice 17 (11) (2009) 1358–1366.
[16] D.Q. Mayne, J.B. Rawlings, C.V. Rao, P.O.M. Scokaert, Constrained Model Predictive Control: stability and optimality, Automatica 36 (6) (2000) 789–814.
[17] T. Alamo, D. Muñoz de la Peña, D.M. Limon, E.F. Camacho, Constrained min–max predictive control: modifications of the objective function leading to polynomial complexity, IEEE Transactions on Automatic Control 50 (5) (2005) 710–714.
[18] J.K. Gruber, D.R. Ramirez, T. Alamo, C. Bordons, E.F. Camacho, Min–Max Model Predictive Control of a pilot plant, in: Proceedings of the 2008 American Control Conference, Seattle, WA, 2008, pp. 1121–1126.
[19] F. Szeifert, T. Chovan, L. Nagy, Process dynamics and temperature control of fed-batch reactors, Computers and Chemical Engineering 19 (1) (1995) 447–452.
[20] D.R. Ramirez, D. Limon, J.G. Ortega, E.F. Camacho, Model Based Predictive Control Using Genetic Algorithms. Application to a Pilot Plant, in:, in: Proceedings of the 1999 European Control Conference, Karlsruhe, Germany, 1999, pp. 81–85.

[21] L.O. Santos, P.A.F.N.A. Afonso, J.A.A.M. Castro, N.M.C. Oliveira, L.T. Biegler, On-line implementation of nonlinear MPC: an experimental case study, Control Engineering Practice 9 (8) (2001) 847–857.
[22] J.H. Lee, K.S. Lee, W.C. Kim, Model-based iterative learning control with a quadratic criterion for time-varying linear systems, Automatica 36 (5) (2000) 641–657.
[23] D.Q. Mayne, S.V. Raković, R. Findeisen, F. Allgöwer, Robust output feedback Model Predictive Control of constrained linear systems, Automatica 42 (7) (2006) 1217–1222.
[24] B. Hu, A. Linnemann, Toward infinite-horizon optimality in nonlinear Model Predictive Control, IEEE Transactions on Automatic Control 47 (4) (2002) 679–682.
[25] D. Limon, T. Alamo, F. Salas, E.F. Camacho, On the stability of constrained MPC without terminal constraint, IEEE Transactions on Automatic Control 51 (5) (2006) 832–836.
[26] J.E. Normey-Rico, E.F. Camacho, Control of Dead-Time Processes, Springer-Verlag, 2007.